INTERNATIONAL JOURNAL FOR NUMERICAL METHODS IN FLUIDS, VOL. 6, 103–112 (1986)

ON NUMERICAL MODELLING OF EMBEDDED SUBSONIC FLOW

M. P. DAVIS

Concentration Heat and Momentum Ltd. 40 High Street, Wimbledon, London SW19 5AU, U.K.

A. C. H. MACE

Royal Armament Research and Development Establishment, Westcott, Aylesbury, Buckinghamshire, HP18 ONZ, U.K.

AND

N. C. MARKATOS

Faculty of Technology, School of Mathematics, Statistics and Computing, Thames Polytechnic, London SE18 6PF, U.K.

SUMMARY

An analytical model has been developed for computing embedded subsonic flow in rocket plumes from underexpanded axisymmetric supersonic nozzles. Numerical procedures based on the analysis have been incorporated in a simplified, non-reacting exhaust structure program and calculations for representative plume conditions performed. The technique is numerically stable and has provided satisfactory predictions of Mach–disc associated embedded subsonic flow.

KEY WORDS Supersonic Subsonic Mach Disc Compressible Pressure-correction

INTRODUCTION

For a gas jet exhausting from an axisymmetric nozzle to a lower pressure surrounding, the flow will follow a Prandtl–Meyer expansion at the corner of the nozzle.[1] The expansion fan will be reflected as compression waves from the constant-pressure jet boundary and subsequently from the jet axis (Figure 1). As the nozzle-exit/ambient pressure ratio is increased the compression waves intersect and coalesce to form a boundary shock wave. Further downstream the compressive effect causes the shock wave to become so strongly curved that regular reflection from the jet axis is not possible; instead a nearly normal shock wave, known as a Mach disc or Riemann wave, occurs. The boundary shock, Mach disc and reflected shock are joined at a triple point and flow downstream of the normal shock becomes locally subsonic (Figure 2).

Axisymmetric non-recirculating rocket exhaust structures can be computed efficiently from time-averaged Navier–Stokes equations by means of marching algorithms.[2,3] These procedures are satisfactory for plumes with underexpansion pressure ratios < 20. However, the techniques employed to evaluate the pressure field in the schemes employed in, for example, References 3 and 4 are, in general, numerically unstable when the volume of Mach-disc associated embedded subsonic flow is comparable with or larger than that of the finite-difference grid cells. This paper is concerned with a method for computing such flow, which can be incorporated within an existing marching-scheme program. The procedures were developed and tested in a GENMIX-derived code.[5] These techniques may be readily incorporated into any marching-scheme rocket-exhaust program with

0271–2091/86/030103–10$05.00

Received 16 January 1984
Revised 9 August 1984

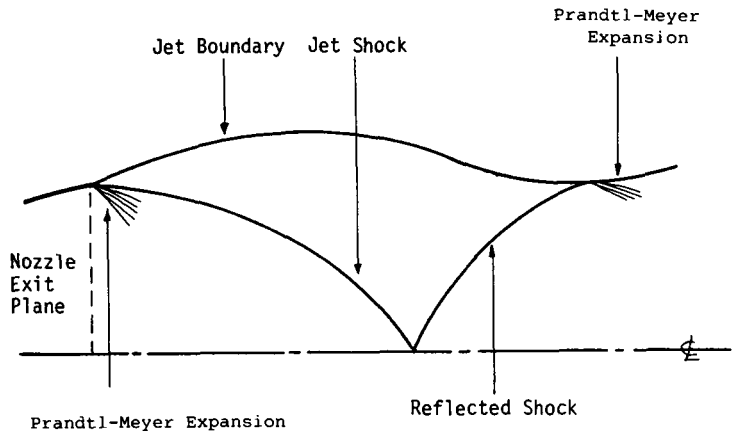

Figure 1. Flow field of a moderately underexpanded exhaust plume

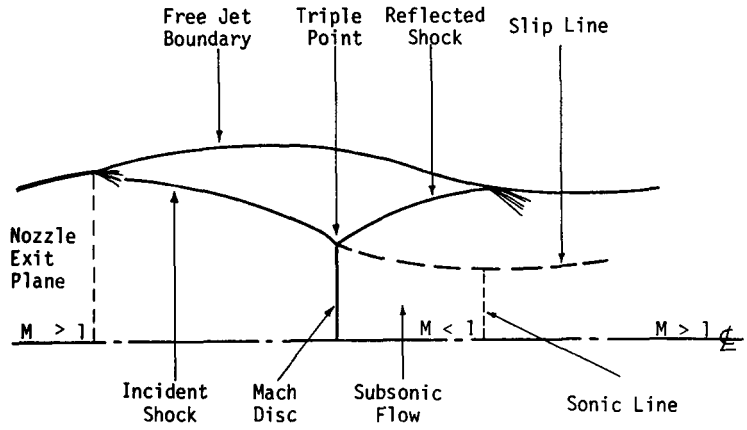

Figure 2. Flow field of a highly underexpanded exhaust plume

provisions to iterate required only in the locality of Mach discs. No widely available spatially resolved data for detailed comparison with the present solution exist. Therefore, the results have still to be validated.

MATHEMATICAL FORMULATION

The conservation equations for momentum, mass and stagnation enthalpy are expressed below in the Von Mises co-ordinate system $(x-\psi)$ for axisymmetric flow.[5]

Conservation of streamwise momentum:

$$\frac{\partial u}{\partial x}=\frac{\partial}{\partial \psi}\left[r^2 \rho u \mu \frac{\partial u}{\partial \psi}\right]-\frac{1}{\rho u}\frac{\partial p}{\partial x} \tag{1}$$

where ψ is the stream function, p is the static pressure, ρ is the density, u is the fluid velocity in the longitudinal direction, μ is the effective viscosity and x and r are the longitudinal and radial distances, respectively. The derivation of the above equation is given in Reference 5.

Conservation of lateral momentum:

$$\frac{\partial v}{\partial x} = -r\frac{\partial p}{\partial \psi} \tag{2}$$

where v is the lateral velocity and viscous terms are omitted.

Conservation of mass:

$$\delta\psi = \rho u r \delta r \tag{3}$$

Equation (3) is used to define the finite-difference grid upon which the conservation equations are solved. The grid uses x–ω co-ordinates in place of x–r co-ordinates, where ω is the dimensionless stream function $\omega = (\psi - \psi_1)/(\psi_E - \psi_1)$, and ψ_1 and ψ_E stand for the stream functions at the internal and external boundaries of the grid respectively.[5] ψ is obtained from equation (3) above.

Conservation of stagnation enthalpy:

$$\frac{\partial H}{\partial x} = \frac{\partial}{\partial \psi}\left[r^2 \rho u \Gamma \frac{\partial H}{\partial \psi}\right] + \frac{\partial}{\partial \psi}\left[(\mu - \Gamma) r^2 \rho u \frac{\partial}{\partial \psi}(u^2/2)\right] \tag{4}$$

where Γ is the effective transport coefficient for stagnation enthalpy (H). Finally, the temperature (T) is computed from the enthalpy, the constant-pressure heat capacity (C_p) and the velocity as $T = (H - u^2/2)C_p^{-1}$, the density is computed from the perfect-gas equation of state, and the Mach number, required in the evaluation of the pressure field, is defined as

$$M = \left[\frac{\rho u^2}{p\gamma}\right]^{1/2} \tag{5}$$

where γ is the ratio of the specific heats.

Equations (1), (2) and (4) provide a means for calculating the principal dependent variables, but provide no guarantee that the continuity equation is satisfied. Equation (3) is satisfied by solving a pressure-correction equation and appropriately modifying velocity and pressure fields so that mass and momentum are conserved simultaneously. The pressure-correction procedures of, for example, References 3 and 4 are unstable in the Mach-disc region and a rigorous treatment of this analysis is required. The pressure-correction equation is derived by requiring that the streamwise cell face areas, computed from the calculated velocities and densities, be the same whether derived from considerations of continuity or of cell geometry.

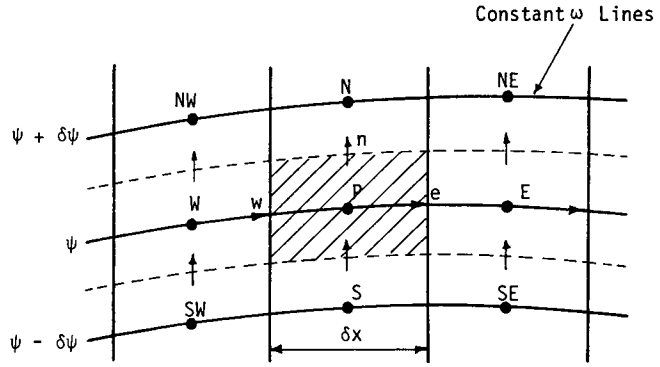

Figure 3. A control volume

Consider the streamtube volume of Figure 3. A conventional staggered-grid is used, according to which velocities are staggered with respect to point P at which all other variables are evaluated. This means that the control cells used for momentum balances are themselves staggered with respect to the cells used for continuity balances and as such they have, in general, different cross-sectional flow areas. Let A represent the flow area associated with the continuity equation and a represent the cross sectional flow area associated with the momentum equation. The compatibility of the cell area is

$$A_e - A_w - E = a_e - a_w \tag{6}$$

where E represents the area increase of A_e associated with entrainment. The 'continuity' areas are, of course, derived from equation (3), e.g. $A_i = \delta\psi_i/(\rho u)_i$, where i stands for e or w. From the geometry of Figure 3 the following relation for the difference in 'momentum' areas can be derived, assuming axisymmetry extending over a sector of one radian.

$$a_E - a_W = \delta x(r_n \tan\alpha_n - r_s \tan\alpha_s), \tag{7}$$

where $\alpha_i = v_i/u_i$. It is appropriate to decompose the quantities u, v, p, ρ, A, a and α into approximate and corrected components such that, for example, the final pressure becomes $p = p^* + p'$. The primed quantities are computed from the pressure-correction analysis and the starred quantities are computed from the solutions to equations (1)–(4). Applying this decomposition to equation (6), recalling that $A_i = \delta\psi_i/(\rho u)_i$ from equation (3), substituting equation (7) for $a_E - a_W$, and ignoring second order u_i' contributions from α_i yields

$$\frac{\delta\psi_e}{(\rho u)_e^* + (\rho u)_e'} - \frac{\delta\psi_w}{(\rho u)_w^* + (\rho u)_w'} - E = \delta x\left[(r_n \tan\alpha_n^* - r_s \tan\alpha_s^*) + \left[\frac{r_n V_n'}{u_n^*} - \frac{r_s V_s'}{u_s^*}\right]\right] \tag{8}$$

where the denominators of equation (8) are expanded to first order in primed quantities. This may be reduced to a form which isolates the cell continuity error ε, as follows:

$$\frac{\delta\psi_e(\rho u)_e'}{(\rho u)_e^{*2}} - \frac{\delta\psi_w(\rho u)_w'}{(\rho u)_w^{*2}} + \left[\frac{r_n V_n'}{u_n^*} - \frac{r_s V_s'}{u_s^*}\right]\delta x = \varepsilon \tag{9}$$

where

$$\varepsilon = \frac{\delta\psi_e}{(\rho u)_e^*} - \frac{\delta\psi_w}{(\rho u)_w^*} - E + \delta x[r_s \tan\alpha_s^* - r_n \tan\alpha_n^*]$$

It is necessary now to construct a method whereby the mass fluxes may be corrected and the error, ε, elliminated. This will be achieved by correcting the pressure field and subsequently re-evaluating equations (1), (2) and (4). Equation (9) may be written in terms of the pressure correction as follows:

$$\begin{aligned}&\frac{\delta\psi_e}{(\rho u)_e^{*2}}\frac{\partial(\rho u)_e}{\partial p_E}(p_P' - p_E') - \frac{\delta\psi_w}{(\rho u)_w^{*2}}\frac{\partial(\rho u)_w}{\partial p_w}(p_w' - p_P') \\ &+ \frac{\delta x r_n}{u_n^*}\frac{\partial v_n}{\partial p_N}(p_P' - p_N') - \frac{\delta x r_s}{u_s^*}\frac{\partial v_s}{\partial p_S}(p_S' - p_P') = \varepsilon\end{aligned} \tag{10}$$

In order to simplify equation (10) let there be coefficients A_I defined as

$$A_I = \frac{\delta\psi_i}{(\rho u)_i^{*2}}\left[\rho_i\frac{\partial u_i}{\partial p_I} + u_i\frac{\partial\rho_i}{\partial p_I}\right], \quad i = e, w;\ I = E, W \tag{11a}$$

and

$$A_I = \frac{\partial x r_i}{u_i^*}\left[\frac{\partial v_i}{\partial p_I}\right], \quad i = \mathrm{n,s}; I = \mathrm{N,S} \tag{11b}$$

Equation (10) may then be reorganized to give

$$p'_P = \frac{A_E p'_E + A_w p'_w + A_N p'_N + A_S p'_S + \varepsilon}{A_E + A_W + A_N + A_S} \tag{12}$$

and the two-dimensional p' field computed as described in the Appendix. The A_I coefficients are simplified further by assuming the fluid to be an isentropic perfect gas. Equation (11a), for the east and west coefficients, then becomes

$$A_I = \frac{\delta\psi_i}{(\rho u)_i^{*2}}\frac{(1+M^2)}{u_i^*}, \quad i = \mathrm{e,w}; I = \mathrm{E,W} \tag{13a}$$

and equation (11b), for the north and south coefficients, reduces, with the aid of equation (3), to

$$A_I = \frac{\delta x^2 r_i}{(\rho u)_i^{2*}\delta r_i}, \quad i = \mathrm{n,s}; I = \mathrm{N,S} \tag{13b}$$

Throughout the analysis local incompressibility has been assumed. The compressible conditions of rocket exhaust plumes were found to be satisfactorily evaluated by weighting the denominator of equation (12) with a factor $(1 + M^2)$ and iterating on all variables including the density. The final converged solutions satisfied momentum conservation and mass-continuity.

NUMERICAL PROCEDURES

The conservation equations for u, v and H were solved by dividing the calculation domain into discrete volumes (Figure 4), integrating equations (1), (2) and (4) over each cell and deriving a set of matrix equations similar to equation (12), but not including the downstream (E) terms.[5] For a given pressure field, solutions to these equations were efficiently evaluated line-by-line using the tri-

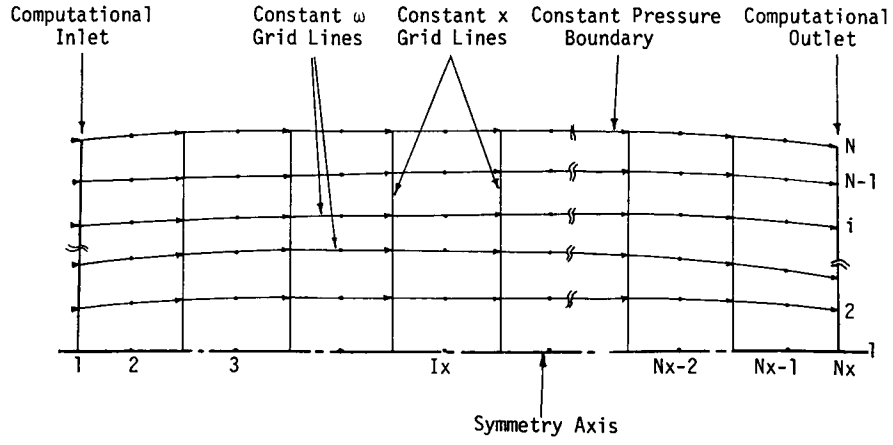

Figure 4. Computational grid

diagonal-matrix algorithm (TDMA).[6] The storage of the variables was therefore one-dimensional. The pressure-correction field was computed by solving equation (12) according to the method described in Reference 7; a summary of this is given in the Appendix. The solutions of equations (1), (2) and (4) and equation (12) were iterated to convergence. Details of the steps involved are as follows:

(i) Initialise inlet conditions and grid variables (Figure 4).
(ii) Calculate boundary conditions: GENMIX symmetry boundary on jet axis,[5] small-wave theory on free-stream boundary.[4,8]
(iii) Move to next axial location in the jet.
(iv) Compute boundary conditions and evaluate new grid.
(v) Solve momentum and enthalpy equations.
(vi) Evaluate temperature, density and Mach number.
(vii) Evaluate the error and A_1 coefficients of equation (12).
(viii) Repeat (iii) to (vii) from inlet to outlet.
(ix) Solve the pressure-correction equation two-dimensionally and correct the pressure field.
(x) Repeat (iii) to (ix) until convergence.

The boundary conditions at the outlet were $\partial v/\partial r = \partial p/\partial x = 0$.

The pressure correction calculated from equation (12) was, for some flows, very large and the iterative cycle (iii)–(ix) occasionally became oscillatory. The pressure was therefore under-relaxed according to the equation

$$p_{\text{new}} = p_{\text{old}} + p' \times R_{\text{f}} \tag{14}$$

where the relaxation factor, R_{f}, was varied between 0·5 and unity.

The algorithm described can be readily incorporated into a conventional marching-scheme program. Plume calculations proceed unchanged from the nozzle exit until a region of embedded subsonic flow is encountered. The program then halts and recommences upstream of the Mach disc following the sequence outlined above. When convergence through the Mach disc region is achieved the program reverts to the non-iterative procedures. The only significant increase in computer storage incurred involves two-dimensional arrays for the pressure, continuity errors and A_I coefficients of the pressure-correction equation through the Mach disc region of the plume.

CALCULATIONS

In order to check the model, the two-dimensional iterative pressure-correction sequence was coded and incorporated in a non-reacting rocket exhaust program derived from GENMIX. For computational ease the turbulence was provided through a fixed effective-viscosity coefficient, $\mu = 0{\cdot}1\,\text{kg m}^{-1}\,\text{s}^{-1}$, and the heat capacities of the inert streams were set to $C_{\text{p}} = 1500\,\text{kJ kg}^{-1}\,\text{K}^{-1}$. Calculations were performed to investigate the capability of computing embedded subsonic flow in rocket exhaust plumes. Results were examined to check numerical stability and physical plausibillity, but the extent to which Mach disc predictions are realistic will need to be re-examined when the procedures are incorporated in fully reacting exhaust structure calculations. Three sets of calculations will be discussed. The first considers how well the new pressure-correction equation computed wholly supersonic flow. Calculations commenced at the nozzle exit-plane and were performed for the conditions given in Table I.

The grid consisted of 20 axial by 11 radial grid nodes uniformly distributed. Calculations, performed with 600 iterations over the calculation domain, converged to give variations $(\Delta\phi/\phi) < 10^{-4}$ between sweeps. Results were compared with a calculation using the procedures

Table I. Nozzle exit plane conditions, case 1

	Jet	Free stream
Velocity (ms^{-1})	2100	2100
Temperature (K)	1400	1400
Pressure (MPa)	1·0	0·1
Jet radius (m)	0·02	

Table II Nozzle exit plane conditions, case 2

	Jet	Free stream
Velocity (ms^{-1})	2100	200
Temperature (K)	1400	300
Pressure (MPa)	2·0	0·1
Jet radius (m)	0·02	

described in References 2–4. This provided a one-dimensional line-by-line marching solution to all variables, including the pressure correction, and was considered adequate for describing wholly supersonic flow.[3,8] Results of computations by the two methods agreed to within 5 per cent, the minor differences being attributed to differing treatments of boundary conditions on adjacent-boundary grid cells.

A second set of calculations studied predictions in the embedded subsonic volume of an exhaust (see Figure 5). Conditions were originally obtained from a marching-scheme calculation based on the conditions given in Table II.

The original calculation failed at 0·7 m and the iterative calculation began at 0·64 m. Again convergence was obtained within 600 sweeps and a region of subsonic flow was predicted between 0·6 and 0·71 m from the nozzle exit. The flow field for the two calculations is illustrated in Figure 5 and the Mach number contours for the second are presented in Figure 6. It is seen that the 2D pressure-correction sequence predicts an immediate contraction of the flow field (Figure 5) simultaneous with the formation of the Mach disc. This structure is seen more clearly in the Mach number contours of Figure 6. The subsonic volume, enveloped by the sonic line, contracts slightly and then forms a tail following the general trend of the contours in this region. Upstream of the Mach disc there is a plateau of high Mach number contours which fall off sharply towards the axis

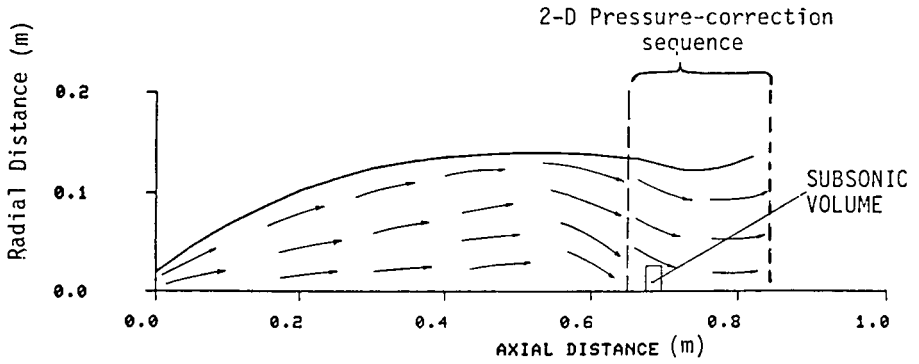

Figure 5. Exhaust flow field showing region of embedded subsonic flow

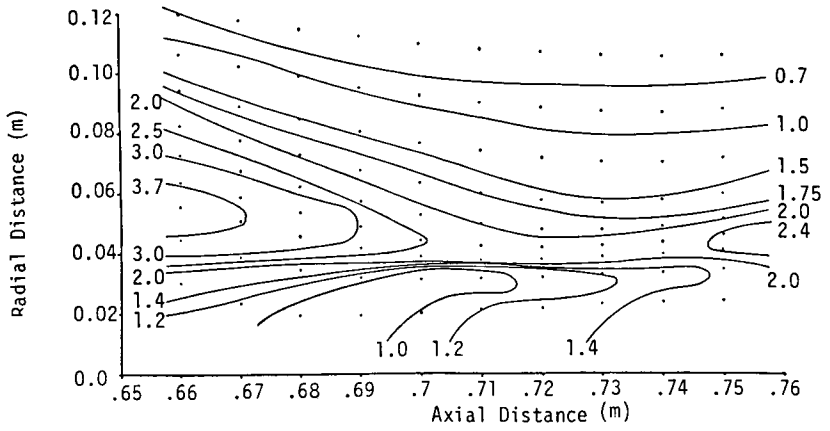

Figure 6. Contours of constant Mach number in locality of embedded subsonic flow

but more gradually towards the free boundary. The highest gradient of Mach number is located near to the tail of the subsonic volume.

Finally, calculations were performed to identify the sensitivity of predictions to variations in inlet data. Results discussed here relate to conditions determined from a marching scheme calculation based on the conditions of Table II but with a nozzle-exit/ambient pressure ratio of 40. A two-dimensional pressure-correction equation calculation converged and predicted a region of subsonic flow from 0·87 to 0·9 m on the jet axis. Although subsequent calculations were sensitive to perturbations in the inlet streamwise-velocity, pressure and temperature distributions, variations were small in comparison with comparable changes to the lateral velocity distribution. To illustrate this, centreline pressure profiles from calculations in which the inlet lateral velocities were scaled by factors 1·0, 1·3, 107 and 1·9 are given in Figure 7. It is seen that an increase in the lateral velocity has the effect of increasing the peak pressure, while moving it closer to the nozzle exit. The transition to subsonic flow not only moved systematically upstream, but the width of the region increased to occupy 50 per cent of the mixing layer width for the factor = 1·9 calculation. In the

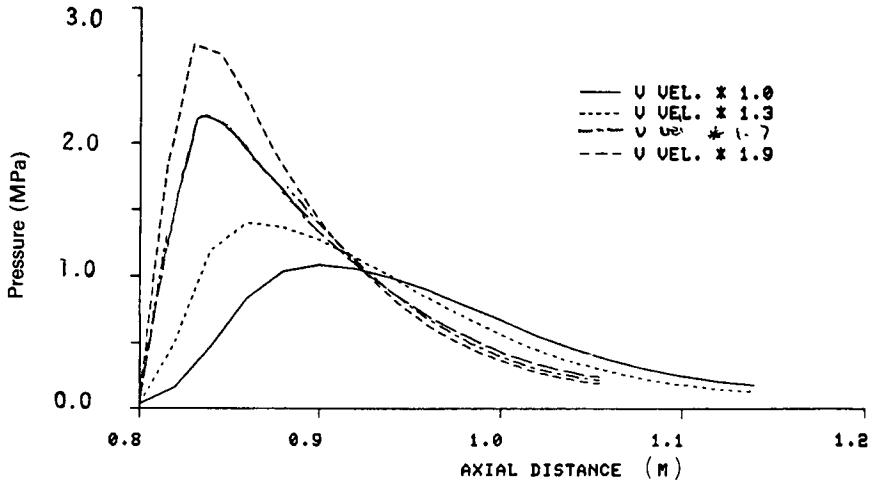

Figure 7. Profile of centreline pressure through the region of embedded subsonic flow showing sensitivity to inlet values of lateral velocity

neighbourhood of Mach discs in rocket exhausts the lateral velocity gradients can be large and the conventional one-dimensional procedures do not provide satisfactory solutions to the momentum equation just upstream of the shock. As it is important that the lateral velocity distribution provided to the two-dimensional pressure procedure is a good solution to the appropriate momentum equation, examination of the velocity fields determines the axial location in the jet where iteration should commence.

CLOSURE

A procedure for computing the velocity and pressure distributions through regions of embedded subsonic flow, as may occur in Mach discs of underexpanded rocket plumes, has been described. The procedure has been coded and incorporated in a simplified rocket exhaust program in which chemical reaction was not considered. Calculations, for conditions similar to those which occur in rocket plumes, have demonstrated that the procedure will compute satisfactorily converged and numerically stable results. The motivation for the work was to develop a technique which would efficiently compute conditions surrounding a rocket plume Mach disc and which may be incorporated in an existing marching solution exhaust structure program. The procedures developed may be exploited in other finite-difference programs dedicated to computing predominantly supersonic flow, but containing regions of embedded non-recirculating subsonic flow.

APPENDIX: SOLUTION OF THE PRESSURE-CORRECTION EQUATION

The pressure correction equation (12) has the form:*

$$A_P p'_P = A_N p'_N + A_S p'_S + A_E p'_E + A_W p'_W + \varepsilon$$

Suppose

$$p'_P = N_P p'_N + E_P p'_E + B_P$$

then

$$p'_S = N_S p'_P + E_S p'_{SE} + B_S$$

and

$$p'_W = N_W p'_{NW} + E_W p'_P + B_W$$

Substitution yields

$$p'_P(A_P - A_S N_S - A_W E_W) = A_N p'_N + A_E p'_E + b + A_S(E_S p'_{SE} + B_S) + A_W(N_N p'_{NW} + B_W)$$

Hence

$$N_P \equiv A_N / D_P$$

$$E_P \equiv A_E / D_P$$

$$B_P \equiv [b + A_S(E_S p_{SE} + B_S) + A_W(N_W p_{NW} + B_W)]/D_P$$

where

$$D_P \equiv A_P - A_S N_S - A_W E_W$$

Therefore the pressure field is obtained as follows:

(i) compute N_P, E_P, D_P starting at low P and stored two-dimensionally
(ii) compute B_P repeatedly using the in-store p'_{SE}; p'_{NW}

*See Figure 3 for subscript identification.

(iii) compute p'_P starting at high P
(iv) repeat until convergence.

REFERENCES

1. M. J. Zucrow and J. D. Hoffmann, *Gas Dynamics Vol.* 1,
2. D. E. Jensen and A. S. Wilson, 'Prediction of rocket exhaust flame properties', *Combustion and Flame*, **25**, 43 (1975).
3. D. E. Jensen, D. B. Spalding, D. G. Tatchell and A. S. Wilson, 'Computation of structures of flames with recirculating flow and radial pressure gradients', *Combustion and Flame*, **34**, 309 (1979).
4. N. C. Markatos, D. B. Spalding and D. G. Tatchell, 'Combustion of hydrogen injected into a supersonic airstream', *NASA CR-2802*, 1977.
5. D. B. Spalding, *GENMIX: A General Computer Program for Two-dimensional Parabolic Phenomena*, Pergamon Press, 1977.
6. F. B. Hildebrand, *Introduction to Numerical Analysis*, 2nd edn, McGraw-Hill, 1974.
7. N. C. Markatos, M. R. Malin and G. Cox, 'Mathematical modelling of buoyancy-induced smoke flow in enclosures', *Int. J. Heat Mass Transfer*, **25**, 63–75 (1982).
8. A. C. H. Mace, N. C. Markatos, D. B. Spalding and D. G. Tatchell,'Analysis of combustion in recirculating flow for rocket exhausts in supersonic streams', *J. Spacecraft and Rockets*, **19**, (6), 557 (1982).